Nonequivalence of the Nucleotide-Binding Subunits of an ABC Transporter, the Histidine Permease, and Conformational Changes in the Membrane Complex†

David I. Kreimer, Krisna P. Chai, and Giovanna Ferro-Luzzi Ames*

Department of Molecular and Cell Biology, Division of Biochemistry and Molecular Biology, University of California, Berkeley, California 94720

Received May 10, 2000; Revised Manuscript Received September 7, 2000

ABSTRACT: The membrane-bound complex of the *Salmonella typhimurium* histidine permease, an ABC transporter (or traffic ATPase), is composed of two membrane proteins, HisQ and HisM, and two identical copies of an ATP-hydrolyzing protein, HisP. We have developed a technique that monitors quantitatively the sulfhydryl modification levels within the intact complex, and we have used it to investigate whether the HisP subunits behave identically within the complex. We show here that they interact differently with various thiol-specific reagents, thus indicating that, despite being identical, they are arranged asymmetrically. The possible basis of this asymmetry is discussed. We have also analyzed the occurrence of conformational changes during various stages of the activity cycle using thiol-specific reagents, fluorescence measurements, and circular dichroism spectroscopy. Cys-51, located close to the ATP-binding pocket, reflects conformational changes upon binding of ATP but does not participate in changes involved in signaling and translocation. The latter are shown to cause secondary structure alterations, as indicated by changes in α-helices; tertiary structure alterations also occur, as shown by fluorescence studies.

The superfamily of ABC transporters (also called traffic ATPases; *1*, *2*) comprises both prokaryotic and eukaryotic membrane transporters that translocate a wide variety of substrates, ranging in size from several atoms to pentapeptides and even proteins. Extensive similarities in the general organization of the various domains and substantial sequence homology in the ATP-binding domain (NBD) is likely to reflect a common mechanism of action. Eukaryotic ABC transporters include medically important systems such as the human cystic fibrosis transmembrane conductance regulator (CFTR), P-glycoprotein (multidrug resistance protein or MDR), the heterodimeric transporter associated with antigen processing (Tap1/Tap2), the presumed cholesterol transporter defective in Tangier disease patients (ABC1, *3*), the retina-specific transporter involved in recessive Stargardt macular distrophy encoded by the ABCR gene, and several others (see ref *4* and references therein). Eukaryotic transporters are usually composed of a single polypeptide chain. In contrast, prokaryotic transporters generally comprise individual polypeptides forming separate domains (*5*). Such a modular architecture has permitted the assignment of separate functions to the various domains through the use of genetic, biochemical, and molecular biological techniques. The most studied prokaryotic members of the superfamily are periplasmic permeases, among which the histidine permease, responsible for translocating L-histidine across the bacterial inner membrane in *Salmonella typhimurium* and *Escherichia coli*, has been extensively characterized (*6*, *7*). This permease, together with another extensively studied bacterial permease, the maltose permease (*8*), provide good model systems for the ABC transporters superfamily.

The histidine permease comprises a membrane-bound complex, $HisQMP_2$, composed of four subunits, two of which, HisQ and HisM, are integral membrane proteins, and two, called HisP, that are identical nucleotide-binding proteins (or domains, i.e., NBDs) with a hydrophilic sequence, yet with a strong tendency to associate with the membrane (*9*, *10*). The energy for translocation is supplied via the hydrolysis of ATP by HisP (*11*−*13*). $HisQMP_2$ (G. F.-L. Ames, manuscript in preparation) and the soluble form of HisP (*14*) have been purified and characterized biochemically. The complete permease system includes, in addition to $HisQMP_2$, a water-soluble receptor, the histidine-binding protein HisJ, which binds the ligand, interacts with $HisQMP_2$, and transmits a signal across the membrane, thus triggering the hydrolysis of ATP by the HisP subunits and ligand translocation (*13*, *15*−*18*). Soluble HisP has been crystallized and its three-dimensional structure has been resolved (*19*). The crystal structure shows a dimer, in agreement with

† This work was supported by NIH Grant DK12121 to G.F.-L.A.

* To whom correspondence should be addressed. Present address: Children's Hospital Oakland Research Institute, 5700 Martin Luther King, Jr. Way, Oakland, CA 94609. Tel. 510-450-7658; fax 510-597-7128; e-mail games@chori.org.

[1] Abbreviations: NBD, nucleotide-binding domain; $HisQMP_2$, the membrane-bound complex containing HisQ, HisM, and two HisP subunits with or without the extension of eight amino acids (Leu-Glu-His-His-His-His-His-His) at the carboxyl terminus; PLS, proteoliposomes reconstituted with purified $HisQMP_2$ complex and subjected to LiposoFast treatment; PLS_{crude}, proteoliposomes not subjected to LiposoFast treatment; W130F, HisJ mutant protein in which Trp-130 is replaced by a phenylalanine; OG, octyl β-D-glucopyranoside; DS, *n*-decanoyl sucrose; SDS−PAGE, sodium dodecyl sulfate−polyacrylamide gel electrophoresis; MIANS, 2-(4′-maleimidylanilino) naphthalene-6-sulfonic acid, sodium salt; PyMPO, 1-(2-maleimidylethyl)-4-(5-(4-methoxyphenyl)oxazol-2-yl)pyridinium methanesulfonate; mBBr, monobromobimane; qBBr, monobromotrimethylammoniobimane bromide; IAEDANS, 5-[(2-iodoacetyl)amino]naphthalene-1-sulfonic acid; NEM, *N*-ethylmaleimide; DTT, dithiothreitol.

10.1021/bi001066+ CCC: $19.00
Published on Web 10/27/2000

biochemical results, and each subunit has two arms in the shape of an L. One of the arms contributes many of the ATP-binding pocket residues and the other contains a region, called the helical domain, that has been postulated to interact with HisQ and HisM (*20*) and is most likely to be involved in the signaling mechanism. Since the liganded soluble receptor binds the membrane-bound complex at the periplasmic aspect, while ATP binding and hydrolysis occur at the inner (cytoplasmic) membrane surface, conformational changes must occur during signaling and/or during ATP hydrolysis and ligand translocation. The transport process can be dissected for practical purposes into the following main steps (*5*, *7*, *21*−*23*): (i) signaling across the transmembrane components upon interaction between the liganded receptor and the membrane-bound complex, via conformational changes propagating from the receptor-binding site(s) to the ATP-binding site(s) in the HisP subunit(s); (ii) induction of ATPase activity in the HisP subunit(s); and (iii) ligand translocation through the complex, which may require additional conformational changes and in which translocation of each ligand molecule appears to be separately coupled to hydrolysis of one ATP molecule (*23*).

Here we have used three approaches, monitoring of thiol-specific chemical labeling, CD spectroscopy, and intrinsic fluorescence measurements, to demonstrate that conformational changes occur during various phases of the transport process. Transmembrane signaling in $HisQMP_2$ is shown to involve clear-cut secondary structure and marginal tertiary structure conformational changes; steady-state ATP hydrolysis is accompanied by substantial tertiary structure conformational changes; and ligand translocation requires tertiary structure conformational changes, which are more pronounced than those accompanying signaling and ATP hydrolysis. The nature of the observed conformational changes is discussed with regard to possible translocation mechanisms.

Since in the case of eukaryotic ABC transporters the NBDs are usually different and have been shown and/or proposed to behave differently, it was of particular interest to determine whether the HisP subunits of the histidine permease, which have identical sequences, also behave differently. This is shown here to be the case, which implies that the NBDs are designed to perform different functions and supports the contention that these prokaryotic systems are appropriate models for the ABC family in general.

EXPERIMENTAL PROCEDURES

Purification of HisJ and $HisQMP_2$ and PLS Preparation. All transport genes are derived from *Salmonella typhimurium*. Unliganded wild-type HisJ is purified as described (*14*), and its concentration is determined by absorbance at 280 nm, using an extinction coefficient of 0.71 for 1 mg/mL protein in a 1 cm path-length cell (*24*). $HisQMP_2$, containing a carboxyl-terminal extension in each HisP subunit (*25*), is purified by use of Talon (Clontech), a metal affinity resin, from membrane vesicles solubilized for 1 h, on ice, in 1% DS (Calbiochem) in buffer containing 10% glycerol, 10 mM $MgSO_4$, 10 mM ATP, 50 mM NaCl, and 50 mM Tris-HCl, pH 8.0 (G. F.-L. Ames, manuscript in preparation). Reconstitution into PLS is performed by dialysis followed by LiposoFast treatment (Avestin Inc., Canada) as described (*17*), using purified $HisQMP_2$ concentrations of 0.6−1.0 mg/mL purified protein. If the LiposoFast treatment is omitted, the PLS are designated as PLS_{crude}. For CD measurements and for occasional labeling experiments as indicated, membranes are solubilized in 1.2% OG (Calbiochem) in buffer containing 20% glycerol, 20 mM $MgSO_4$, 10 mM ATP, 50 mM MOPS, pH 7.5, and 10 mg/mL total *E. coli* lipid extract (Avanti Polar Lipids, Inc.) (*25*) and reconstituted in PLS as described (*18*) with 0.1−0.2 mg/mL purified protein. Transport and ATPase activities are determined as described (*17*, *18*); occasionally, as indicated, the $MgSO_4$ and ATP concentrations are 2 mM each. When PLS are to be used for thiol-specific modification experiments, dithiothreitol (DTT) is omitted from the last two changes of the dialysis buffer (with no effect on the ATPase and transport activities). PLS_{crude} obtained from DS-solubilized $HisQMP_2$ are impermeable to HisJ but permeable to low molecular weight compounds, such as MgATP and sulfhydryl-modifying reagents. PLS obtained from OG-solubilized $HisQMP_2$ are impermeable to both HisJ and low molecular weight compounds (*17*).

Site-Directed Mutagenesis and Purification and Characterization of Mutant HisJ Protein W130F. Trp-130 in HisJ was changed to a Phe residue by in vitro mutagenesis of plasmid pFA54 [which carries the *hisJ* gene under the control of the TAC promoter (*26*)] to give plasmid pFA297, which contains the *hisJ* gene carrying the Phe-130 codon. Plasmid pFA297 was introduced into TG1 cells by electroporation and the entire *hisJ* gene was sequenced to ascertain the presence of the mutation and the absence of PCR errors. pFA297 was then electroporated into TA2918 (*dhuA1 hisF*Δ645 *hisJ*Δ6776), yielding strain GA665, which allows assay of the properties of the mutant receptor in vivo. The mutant protein thus encoded, W130F, was purified to 98% purity from GA665 cells employing essentially the same protocol as for wild-type LAO, with 5 mM Tris-HCl buffer, pH 8.3 (*27*). The final DEAE HPLC column was washed extensively (1.5 h, 5 mL/min) with 5 mM Tris-HCl buffer, pH 8.3, which removes the endogenous ligands (*27*), prior to elution with a NaCl gradient from 0 to 300 mM. A single peak of W130F was eluted at 185 mM NaCl (wild-type HisJ is eluted at 17 mM NaCl). Tyrosine intrinsic fluorescence titration upon addition of L-histidine confirmed that W130F was unliganded. Protein concentration was determined by the Lowry method (*28*), with wild-type HisJ as a standard. The affinity of W130F toward L-histidine was characterized by equilibrium dialysis employing radiolabeled L-histidine (L-[^{3}H]histidine, Amersham Corp.) (*29*). The apparent K_d value for the complex of L-histidine-liganded W130F and $HisQMP_2$ was estimated from the dependence of the ATPase activity in $HisQMP_2$ on receptor concentration (*21*).

Fluorescence and CD Measurements. For intrinsic fluorescence measurements PLS_{crude} are frozen/thawed 5 times in a liquid nitrogen/water bath at 25 °C to equalize the exterior and interior environment of PLS_{crude}. Measurements are performed on a Hitachi-4000 spectrofluorometer equipped with a thermostated cell holder, at 24 °C, in a 1.0 × 1.0 or a 0.3 × 0.3 cm cuvette with the slits for excitation and emission both set at either 5 or 2 nm. The excitation wavelength is 296 nm unless otherwise stated. For measurements of the intrinsic fluorescence quenching by I^-, samples are prepared at various KI concentrations using a fresh solution

of 3 M KI and 1 mM $Na_2S_2O_3$ (to prevent the formation of I^-) in water. The total ionic strength corresponding to the maximum KI concentration used in the experiments (0.3 M) is maintained constant by corresponding amounts of KCl. Measurements are performed at 24 °C immediately after the last thawing, before any substantial accumulation of the products of ATP hydrolysis. All fluorescence spectra are corrected for the contribution due to the corresponding buffer. The fluorescence intensity obtained for $HisQMP_2$ in the presence of W130F is corrected by subtraction of the intensity of W130F (with and without ligand) at each KI concentration. The fluorescence intensity of the corrected spectra at 337 nm is used to construct Stern−Volmer plots.

CD measurements are performed with PLS reconstituted from OG-solubilized $HisQMP_2$. An Aviv 62DS spectropolarimeter equipped with a thermostated cell holder is employed. Spectra are recorded at 25 °C, with a 0.01 or 0.02 cm path-length cuvette, in the wavelength range 186−250 nm at 0.2 nm intervals, at a scan rate of 20 nm/min. Experimental data representing the average of 8 scans are expressed in millidegrees and are corrected for the contribution due to the corresponding buffer. The absolute value of ellipticity for $HisQMP_2$ is calculated from a protein concentration value obtained by a modified Lowry method (*30*) with bovine serum albumin as a standard.

Chemical Modification with SH Reagents. The sulfhydryl reagents employed are PyMPO, mBBr, MIANS, IAEDANS, qBBr, NEM, and $HgCl_2$ (all from Molecular Probes, Inc., Eugene, OR, except for NEM and $HgCl_2$, which were obtained from Sigma). The first four are charged (either positively or negatively) and penetrate hydrophobic regions poorly (*31*). All these reagents, except for NEM and $HgCl_2$, are or become fluorescent upon derivatization. mBBr generates upon reaction the smallest fluorescent moiety (molecular mass 271); qBBr has a similar structure and utilizes the same chemistry of modification but is positively charged. IAEDANS utilizes similar chemistry of modification but is substantially larger (molecular mass 434) and is negatively charged. MIANS (molecular mass 416) has a structure similar to that of IAEDANS and is also negatively charged but utilizes its maleimide group for modification. PyMPO (molecular mass 471), which is only slightly larger than MIANS and utilizes the same maleimide chemistry, is positively charged. Thiol-specific modification is performed in the dark, with 0.5 mL of PLS or PLS_{crude} containing 0.6 mg/mL protein, in 50 mM Tris-HCl buffer, pH 8.0, preequilibrated at 44 °C. The presence of 100 mM NaCl did not change the results. When mBBr, IAEDANS, or PyMPO is used, the reagent is added to a final concentration of 2, 2, or 0.8 mM, respectively (unless otherwise stated), and the reaction is allowed to proceed at 44 °C for 40 or 120 min. When MIANS, qBBr, or NEM, each of which is unstable in water (*31*), is used, fresh reagent is added every 5 min in 10 aliquots, each aliquot yielding a final concentration of 0.2, 1.0, and 1.0 mM, respectively, to reach a calculated total of 2, 10, and 10 mM, respectively. Modification by $HgCl_2$ (1 mM) is for 40 min at 44 °C, although this reagent almost instantly eliminates ATPase activity (see text). The reactions are monitored by removing aliquots (10 μL) at various times and mixing them with 1 μL of a quenching solution (1.0 M DTT and 10% SDS), followed by resolution by SDS−15% polyacrylamide gel electrophoresis in the absence of β-mercaptoethanol (unless otherwise stated), with the pH of the resolving gel adjusted to 8.45 (*32*). The resolved gel is washed four times (15 min each) in 50% methanol, to remove low molecular weight products of the modifying reagent (*33*), and if the reaction yields fluorescent derivatives, fluorescence in the gel is excited on a UV light box (FOTO/UV26, Fotodyne). The image is collected through a Petri dish filled with a 4% solution of $CuSO_4$ in water (1.5 OD units at 800 nm), which acts as a filter that is not transparent to the excitation light, and quantified by an IS-1000 Digital Imaging System (Alpha Innotech Corp.). The degree of modification[2] within each band is expressed as a percentage of the fully modified denatured $HisQMP_2$ subunits. Fully modified denatured samples (=100% labeling) are prepared by centrifuging an aliquot of PLS or PLS_{crude} in an Airfuge (Beckman) in an ice-cold rotor for 10 min, solubilizing the pellet in 1% SDS, 8 M urea, and 50 mM Tris-HCl, pH 8.0 (SDS/urea) for 30 min at 24 °C, adding modifying reagents (50 μM), and incubating for 20 min, at which time the reactions have reached completion. Raw band fluorescence values are corrected by subtracting background fluorescence and normalized to the mean fluorescence in the completely modified samples (in triplicate) also corrected for the background. MIANS modification is also monitored continuously by adding MIANS or buffer directly to a PLS-containing solution in a 1.0 × 1.0 cm or in a 0.3 × 0.3 cm cuvette equilibrated at 37 or 44 °C in the thermostated cell holder of the spectrofluorometer and by recording continuously the fluorescence at 440 nm (*31*). Both slits are set at 10 nm, and the excitation wavelength is 330 nm. The kinetics of modification is linear for the first 5 min.

8-Azido-ATP Labeling of PyMPO-Modified PLS. PLS_{crude} (400 μL, 0.6 mg of protein/mL) are treated with 0.8 mM PyMPO for 25 min at 44 °C, followed by quenching with 0.2 M DTT. DTT, which interferes with 8-azido-ATP labeling, is removed by addition of 4 mL of 50 mM Tris-HCl, pH 8.0, and centrifugation for 15 min at 45 000 rpm in a Beckman TL ultracentrifuge. The pellet is resuspended in 4 mL of 50 mM Tris-HCl buffer, pH 8.0, ultracentrifuged for 15 min, and resuspended at a final protein concentration of 0.6 mg/mL. 8-azido-ATP (Sigma) is added to 0.2 mL of this preparation to a final concentration of 0.07 mM, followed by UV irradiation with a short-wave, 254 nm UV lamp (Ultraviolet Products, San Gabriel, CA), as described (*34*). Aliquots are removed at 0, 5, 30, 60, 120, and 240 s and subjected to SDS−PAGE, and an image of the fluorescence of the gel is obtained as described above.

RESULTS

Thiol-Specific Labeling. Sulfhydryl reagents are useful in a variety of ways to help understand the structure and function of proteins because of the specificity of the sulfhydryl modification reaction (*35*). They allow investigation of the accessibility of particular protein areas (*36*−*38*), characterization of the sulfhydryl environment (*39*−*42*), manipulation of the protein stability (*43*−*45*), and incorpora-

[2] The fluorescence intensity of water-soluble proteins as determined from SDS−polyacrylamide gel bands has been shown generally to be proportional to the number of modified thiol groups (see ref *33* and references therein). Since membrane proteins may retain some tertiary and secondary structure in the presence of SDS, the ratio of derivatized SH groups in HisQ, HisM, and HisP does not necessarily correspond to the ratio of the actual number of the respective SH groups.

tion of steric hindrance (*37*, *38*). Of particular interest for this project have been thiol-specific reagents that can be used to analyze protein structure and protein conformational changes (*31*, *46*, *47*). A number of such reagents yield fluorescent derivatives, which are particularly useful for monitoring continuously the reaction progress. In $HisQMP_2$ there is a total of six cysteines: one in each HisP subunit, Cys-51; one in HisQ, Cys-197; and three in HisM, Cys-104, Cys-114, and Cys-149 (*48*). None of these cysteines is conserved among ABC transporters (*10*, *20*), suggesting that they do not perform an essential function. Disulfide bonds in $HisQMP_2$ appear to be absent because the mobility of each of the subunits, HisQ, HisM, and HisP, in SDS−PAGE in the presence and absence of β-mercaptoethanol does not change (data not shown). Treatment of $HisQMP_2$ in PLS_{crude} by denaturation in SDS/urea in the presence and absence of 2 mM DTT at pH 8.0 (1 h, 24 °C), followed by treatment with MIANS, IAEDANS, mBBr, or PyMPO (at final concentrations of 1 and 5 mM in the absence and presence of DTT, respectively), results in identical levels of modification of all the denatured subunits regardless of whether DTT is present; the maximum modification level is reached for all subunits at 20 min and no further change is seen after incubation for 40 or 60 min. The inability to detect disulfide bonds is consistent with the topological prediction in the case of HisM; its membrane-spanning domain containing Cys-104 and Cys-114 is predicted to be in an α-helix within the lipid bilayer (*10*), which would make it unlikely that they form a disulfide bond either between each other (because energetically unfavorable bending and twisting of the α-helix would be required) or with Cys-149, which is in the hydrophilic cytoplasmic loop. In the crystal structure of HisP the only cysteine residue, Cys-51, is buried and is too far from the Cys-51 in the other subunit to form a disulfide bond (*19*). Thus, none of the cysteine residues is engaged in a disulfide bond, and therefore, all of them should be rendered accessible to sulfhydryl reagents under suitable conditions, even without treatment with a reducing agent.

Modification with Sulfhydryl Reagents. mBBr is a small hydrophobic molecule that modifies protein thiols readily (*49*; see also ref *31* and references therein). Its ability to react with $HisQMP_2$ was tested at various temperatures. Incubation of PLS_{crude} (which are permeable to reagents comparable in size to ATP; G. F.-L. Ames, manuscript in preparation) with mBBr, as described under Experimental Procedures, results in 100% modification of HisM, 50% modification of HisQ, and no modification of HisP when performed at 23 °C; raising the incubation temperature to 34 °C (for 2 h) increases the level of HisQ modification to 80% and that of HisP to 17% (Figure 1A). At 44 °C the modification level is 100% for all three subunits (data not shown).[3] An Arrhenius plot summarizing the results of chemical modification at various temperatures shows that the slope is steeper for HisP than that for HisQ, which is steeper than that for HisM (Figure 1B), indicating a substantially higher Arrhenius energy barrier for Cys-51 in HisP. This may indicate either that Cys-51 is in an environment which maintains an abnormal p*K* of its SH group or that it is buried in a tightly packed surrounding. Because

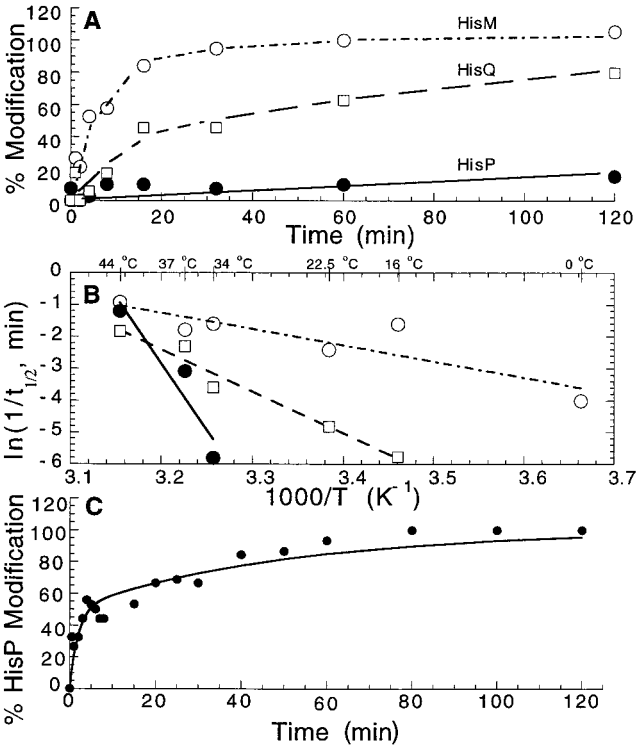

FIGURE 1: Kinetics of chemical modification of $HisQMP_2$ by mBBr. The modification in PLS_{crude} of HisP (●), HisQ (□), and HisM (○) and quantitation were performed as described under Experimental Procedures. (A) Time course of modification at 34 °C. Modification levels are expressed as percent of the modification level of the respective fully modified component. The error in fluorescence band quantitation is ±5%. (B) Arrhenius plots for the modification reactions. Modification was performed and quantitated as described for panel A. The error in the determination of the half-times for modification for each subunit, $t_{0.5}$ (minutes), was ±20%, except for HisP at 34 °C, which was ±50%. It is technically difficult to obtain more data point for HisP because of the very low level of modification at the lower temperatures, even upon prolonged incubation; the value for HisP modification at 34 °C has therefore been obtained by extrapolation. HisQ modification at 0 °C was marginal. (C) Kinetics of modification of HisP in $HisQMP_2$. The modification was performed at 44 °C and monitored as described for panel A. The percentage of HisP modified is plotted versus time and best-fitted (GraFit 3.0 program) by the curve $y = 1 - 0.5\exp(-0.50t) - 0.5\exp(-0.02t)$, which corresponds to the independent modification at different rates, 0.5 and 0.02 min^{-1}, of the two HisP subunits.

the rate of modification of HisP is essentially the same at pH 8.5 and 7.5 (data not shown), the p*K* value may not be a factor and the latter possibility appears more likely. The fact that in the HisP crystal structure Cys-51 is completely buried (*19*) provides the most likely explanation for the high energy barrier for its modification. The modification of HisP at 44 °C could be quantitated separately from that of HisQ and HisM. The time curve of modification (Figure 1C) is biphasic, with half the level of modification being reached within the first 5 min, after which time the reaction proceeds much more slowly, reaching 100% after 2 h. Such a biphasic reaction rate suggests that the two cysteines in HisP have different reactivities, with one of them being readily accessible and the other one considerably less so. Below we provide additional evidence for differences in HisP reactivities.

Sulfhydryl reagents with properties different from those of mBBr were then tested under the same conditions of full

[3] It should be noted that transport (*18*) and ATPase activities are not impaired by incubation of the complex at 44 °C for up to 4 h.

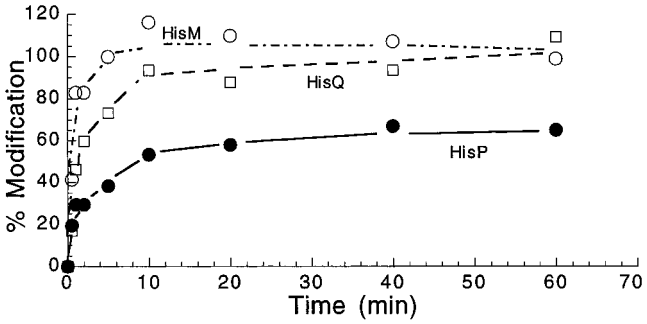

FIGURE 2: Time course of modification of $HisQMP_2$ subunits by PyMPO. Modification and monitoring of the reaction were performed as described under Experimental Procedures and in the caption to Figure 1A. The error in fluorescent band quantitation was ±5%.

labeling. PyMPO, which is positively charged and larger than mBBr, modifies HisQ and HisM to 100% but modifies only about half of HisP (Figure 2). Raising the PyMPO concentration, making repeated reagent additions, or prolonging the incubation time increases the level of HisP labeling slightly, but 100% modification is not achieved within 4 h and at concentrations up to 2 mM PyMPO.

Experiments were designed to exclude the possibility of artifacts resulting in partial HisP labeling. The possibility that the $HisQMP_2$ population is heterogeneous is unlikely because the results are the same under a variety of conditions, including different purified batches of $HisQMP_2$, reconstitution in PLS_{crude} or PLS, and a wide variation in the lipid concentration during reconstitution (data not shown). Other possible explanations are that half of the cysteines have been chemically altered in the course of PyMPO treatment and have become unreactive or that both cysteines react with PyMPO but half of the modified residues are not fluorescent. These possibilities were excluded by various experiments. A mild treatment, i.e., exposure to 1% DS or OG, which does not change the activity of the complex and is very unlikely to change the chemical reactivity of the cysteines, allows 100% modification with PyMPO (40 min at 44 °C). The presence of 15 mM $MgCl_2$ also results in 100% modification. The unmodifiable SH groups are available to other reagents even after PyMPO treatment and thus are unreacted. This was shown by exposing a preparation, in which HisP had been modified with PyMPO to the 50% level, to MIANS for 20 min at 44 °C; the PyMPO-labeled HisP band acquired additional fluorescence, corresponding to a 50% level of modification by MIANS, indicating that the 50% of the sulfhydryls that are not modified by PyMPO remain accessible to other reagents.

An important explanation of this phenomenon would be that since only half of the HisP molecules has been shown to face the exterior in PLS (*18*), PyMPO, being impermeant, would only label these externally exposed molecules. However, the PLS_{crude} used in these experiments are permeable to ATP (G. F.-L. Ames, manuscript in preparation) and therefore PyMPO should also be able to access the interior. To completely exclude the possibility that limited permeability is involved, PLS were also used. PLS are fully impermeable to ATP, HisJ, L-histidine, and carboxyfluorescein (*17*, *18*) and to dipicolinic acid (G. F.-L. Ames, manuscript in preparation) and presumably to PyMPO. If impermeability of PLS_{crude} were the problem, then labeling

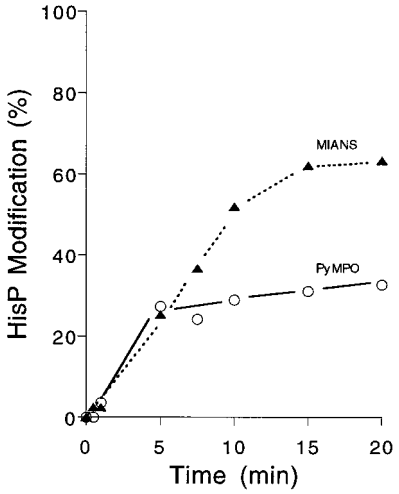

FIGURE 3: Kinetics of HisP modification by PyMPO (○) and MIANS (▲) in PLS. Modification and monitoring were performed in PLS as described under Experimental Procedures and in the caption to Figure 1A. PLS are completely impermeable to charged reagents under the conditions of the experiment. The error in fluorescent band quantitation was ±5%.

in PLS should allow the same labeling level as PLS_{crude}. However, while MIANS modifies half of HisP, as would be expected for an impermeant reagent [MIANS is comparable to PyMPO in size, charge (although it is negatively charged), and has the same chemistry of modification] (Figure 3, ▲ and ○, respectively), only about a quarter of HisP in PLS is labeled with PyMPO. Thus, PyMPO labels only half as many of the accessible HisP molecules as can be labeled with MIANS. This supports the contention that only half of the accessible HisP is PyMPO-modifiable.

Finally, it should be noted that the phenomenon of partial modification is not peculiar to PyMPO because another positively charged SH reagent, qBBr, also modifies only 50% of HisP in PLS_{crude} upon incubation at 44 °C (data not shown). As additional controls, treatment of PLS_{crude} with other sulfhydryl reagents, such as MIANS (see later) and IAEDANS (data not shown), which are also charged, although negatively, and also larger than mBBr, modified all subunits to 100%. In conclusion, it appears that permeability is not an issue and that the two HisP sulfhydryls indeed behave differently in their reactivity to PyMPO, qBBr, and mBBr.

The reactivity of the PyMPO-modified protein was also tested with an entirely different type of reagent, the photoreactive ATP analogue 8-azido-ATP. This reagent also labels only 50% of HisP in $HisQMP_2$ (*32*, *34*, *50*), which is consistent with the notion that the two subunits are different in the complex. By use of the decreased mobility of 8-azido-ATP-modified HisP in SDS−PAGE as an assay (*50*), 8-azido-ATP was confirmed to modify HisP up to a maximum of 50%. To determine whether the selectivity of 8-azido-ATP labeling is the same as that of PyMPO, PyMPO-modified HisP (to the 50% level) was treated with 8-azido-ATP and resolved by SDS−PAGE. Two bands are obtained and both are fluorescent: a lower one at the position of unmodified HisP and PyMPO-modified HisP, and an upper one of lower mobility at the position of 8-azido-ATP-modified HisP (data not shown). Thus, the upper band must contain two forms of HisP, one modified with 8-azido-ATP and the other with both 8-azido-ATP and PyMPO; the lower

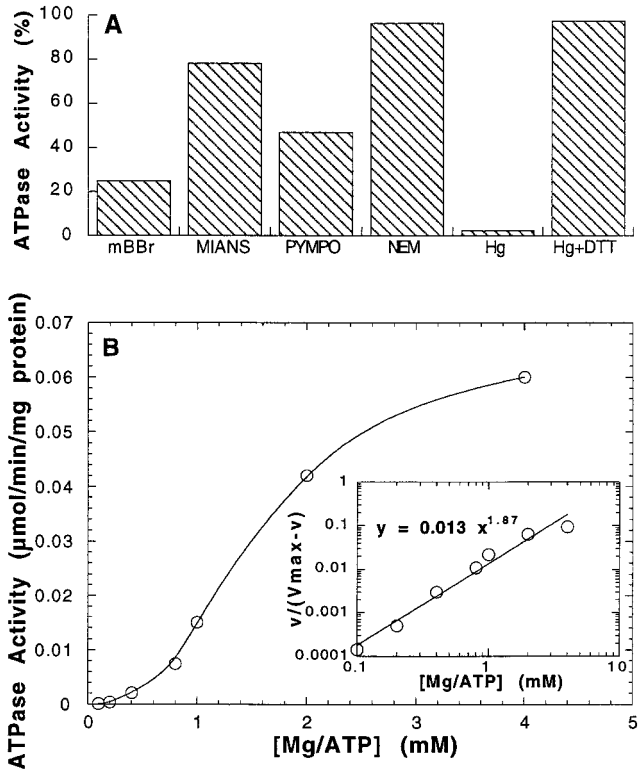

FIGURE 4: Effect of sulfhydryl modification on the ATPase activity. (A) The ATPase activity was assayed as described under Experimental Procedures after treatment of $HisQMP_2$ in PLS_{crude} with the indicated reagents for 40 min in each case. The extent of modification by NEM and $HgCl_2$, which yield no fluorescence, is unknown. The ATPase activity is expressed as a percentage of the activity in the nonmodified sample. The error was ±5%. The products of the modification reaction are present in the ATPase assay mixture, except in the case of $HgCl_2$, which has been removed by extensive dialysis prior to assaying of the activity. Addition of DTT (100 mM, 5 min at room temperature) to the $HgCl_2$ modification reaction mixture reverses the inhibition almost completely. (B) ATPase activity of PYMPO-modified $HisQMP_2$ as a function of ATP concentration. The $MgSO_4$ concentration was adjusted to be always 10 mM above the ATP concentration (*18*). The inset shows that the Hill coefficient is 1.87.

band must contain unmodified HisP and PyMPO-modified HisP. Thus, the basis for the partial modification by 8-azido-ATP is different from that dictating PyMPO modification. In conclusion, the fraction of the sulfhydryls not modified by PyMPO remains chemically intact.

Correlation between Sulfhydryl Modification and ATPase Activity or Cooperativity for ATP. To use these reagents for the study of conformational changes, it is necessary that the modification does not disrupt excessively the protein structure. In the previous section it was shown that PyMPO does not alter drastically the ATP-binding pocket, because the ability to bind and react with the ATP analogue is maintained. The ATPase activity, used as a sensitive indicator of an undisturbed structure, was assayed in $HisQMP_2$ modified with MIANS, and the level of modification was determined simultaneously by the continuous fluorescence assay. A complex fully modified with MIANS retains 80% of the ATPase activity (Figure 4A); the same is true upon modification with NEM (20 mM),[4] as was also shown previously (*18*). Modification with PyMPO, under conditions of complete labeling of HisQ and HisM and about half of HisP, results in about 50% loss of ATPase activity. $HgCl_2$ and mBBr inhibit more extensively. Although $HgCl_2$ yields total inhibition, it does not appear to damage the protein irreversibly, because the inhibition can be completely reversed by DTT (Figure 4A).

The possibility that the 50% loss of activity observed in PyMPO-modified HisP might reflect the complete modification and consequent inactivation of one of the two subunits in a dimer can also be investigated by determining whether the modified protein retains positive cooperativity for ATP (*14*, *18*). If the 50% inhibition of ATPase activity upon labeling with PyMPO (when 50% of HisP is modified) were due to complete inactivation of one of the two HisP subunits, the cooperativity for ATP should be eliminated (*23*). Figure 4B shows that the ATPase activity of the modified protein retains cooperativity, which indicates that both subunits have retained activity. It appears that the modification decreases the activity of each of the subunits of the dimer by 50%, even though only one subunit is modified.

In conclusion, the modification of cysteines can result in various levels of inhibition depending on the nature of the modifying moiety, the residual activities are not directly correlated with the extent of modification, and cooperativity is retained. These results demonstrate that the cysteine residues of HisP are not essential for hydrolysis and that their modification does not disrupt the structure drastically. At the same time, the changes in ATPase activity suggest that these residues and their environment are sensitive to structural rearrangements. In particular, MIANS modifies all subunits of $HisQMP_2$ completely while maintaining an almost unaltered activity level and is therefore a good candidate for the analysis of conformational changes.

Detection of Conformational Changes. The ability to monitor quantitatively the modification of the various components of the complex was used to start an investigation of conformational changes during a cycle of activity. Under steady-state conditions, various conformational species of $HisQMP_2$ should coexist at concentrations that depend on their respective life spans. As the system is locked in a particular operational state, the relative proportions of some of these conformational species change. Such a shift might be detected by a variety of measurements. Several such operational states can be generated individually in this system: (i) signaling by unliganded or liganded receptor [at the periplasmic (external) membrane surface] in the absence of ATP (abortive signaling); (ii) signaling by liganded or unliganded receptor at the periplasmic surface, resulting in induction of ATP hydrolysis by HisP at the cytoplasmic (inner) membrane surface (productive signaling); (iii) binding of ATP to HisP at the cytoplasmic membrane surface in the absence of receptor. Having established the useful characteristics of MIANS modification of the complex, an analysis of various conformational changes at several states was performed with this reagent. These thiol modification experiments were then supplemented by studies with far-UV CD, intrinsic tryptophan fluorescence analysis, and quenching of tryptophan fluorescence.

HisP Undergoes a Conformational Change in the Presence of ATP As Detected by Sulfhydryl Modification. The rates

[4] It is most likely that NEM modifies all cysteines under these conditions because it is less bulky than MIANS and mBBr and it is used at a 10-fold higher concentration.

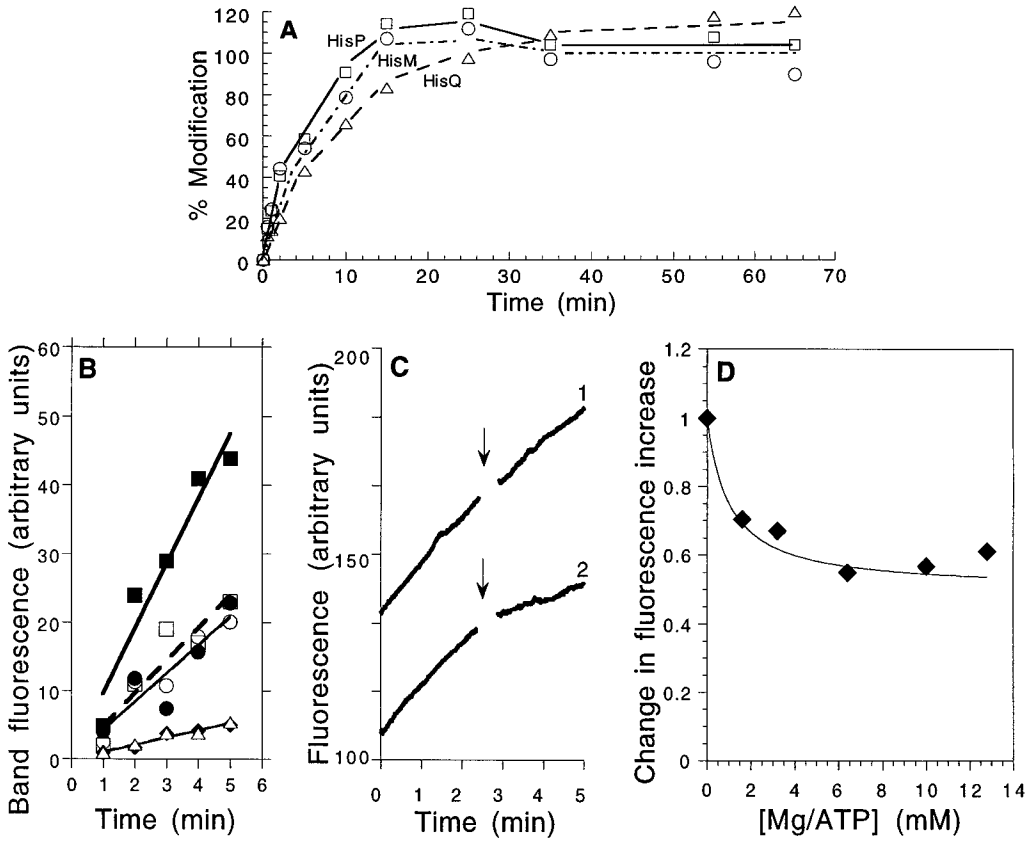

FIGURE 5: Conformational changes in MIANS-modified $HisQMP_2$. Modification by MIANS and quantitation was performed as described under Experimental Procedures. (A) Time course of modification of the individual subunits, with the level of modification expressed as a percentage relative to a totally labeled sample: HisP, squares; HisM, circles; HisQ, triangles. (B) Effect of ATP on the kinetics of modification of the individual subunits. A single addition of MIANS at the final concentration of 0.2 mM was made in the presence (solid symbols) or absence (open symbols) of 10 mM MgATP. (C) Continuous assay of $HisQMP_2$ modification, with and without ATP. The formation of fluorescent MIANS−protein conjugate was monitored continuously as described under Experimental Procedures, for 2 min, at which time 10 μL of 10 mM ATPMg was added to the cell containing 200 μL of reaction mix, and the reaction was monitored for 2 min more (curve 2). As a control, 10 μL of buffer was added to an identical reaction mix (curve 1). The ordinate of curve 2 is shifted for ease of comparison. (D) Effect of varying the Mg/ATP concentration on the modification reaction. Various concentrations of Mg/ATP were added (abscissa) and the level of modification was analyzed as described in panel C. The change in the rate of modification is expressed as the relative change in the slope of the fluorescence kinetics as determined at time intervals from 1 to 2 min and from 3 to 4 min. The curve, generated by the KaleidoGraph program, is the binding isotherm characterized by a K_d value of 1.0 ± 0.4 mM (and a final level for the change in fluorescence increase rate of 0.50 ± 0.05). The results shown in Figure 5C,D were obtained in a single experiment; two other independent experiments gave essentially the same results.

of labeling of the individual subunits of $HisQMP_2$ with MIANS were determined by quantification of the fluorescence of the individual protein bands upon resolution by SDS−PAGE. The subunits display somewhat different initial rates of labeling, although they all reach full labeling within 25 min (Figure 5A). The initial rate of modification of HisP is decreased by about 50% in the presence of MgATP (Figure 5B, ■ and □), whereas there is no significant change in the rates of modification of HisQ ▲ and △) and HisM (● and ○). The rate of labeling was also monitored continuously by following the time-dependent fluorescence increase. This method has the advantage of being considerably more sensitive than analysis of fluorescence in SDS−PAGE (discontinuous assay); however, it does not discriminate between the individual subunits. Figure 5C shows that, upon addition of MgATP, the overall modification rate decreases and the decrease is consistent with the 50% decrease in labeling of HisP shown in Figure 5B (assuming that the fluorescence intensities of the subunits are the same in the two assays). The apparent affinity for MgATP with respect to its effect on MIANS labeling was determined to be approximately 1 mM (Figure 5D). This value is similar to the K0.5 value of 0.6 mM measured for the affinity of the ATPase for ATP (18). These results indicate that accessibility of Cys-51 to MIANS decreases in the presence of ATP, presumably as a consequence of a conformational change occurring in HisP upon binding ATP. A possible effect of signaling by the HisJ receptor or by ATP hydrolysis on the rate of modification was also tested. No additional changes were observed on the rate of the sulfhydryl modification if either liganded or unliganded HisJ was added in the presence of ATP, as determined by both continuous and discontinuous measurements (data not shown).[5] Neither did the addition of receptor in the absence of ATP have any effect on the rate of MIANS and IADEANS labeling (data not shown). Thus, HisP undergoes conformational changes that involve Cys-51 upon binding ATP. Signaling, either abortive or productive as

[5] Since the two cysteine residues in HisJ are engaged in a disulfide bridge (*51, 52*) and therefore are inaccessible to sulfhydryl reagents under nonreducing conditions, they do not contribute to the MIANS modification results.

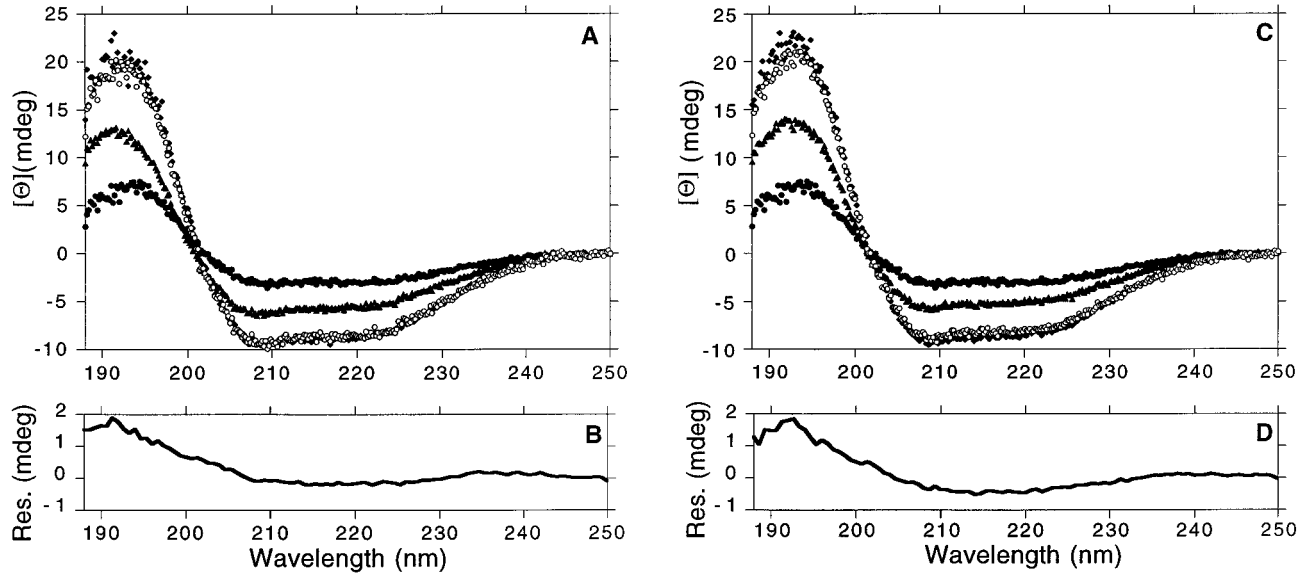

FIGURE 6: Far-UV CD spectra of PLS in the presence and absence of liganded and unliganded HisJ. The final concentrations of the reagents, when present, are (in 50 mM $NaPO_4$ buffer, pH 8.0): $HisQMP_2$, 1 μM (in PLS prepared from OG-solubilized membranes); P lipid, 3 mg/mL; HisJ, 25 μM. Spectra were collected from a 0.01 cm path-length cell. All experimental spectra are corrected for the corresponding buffer baseline. (A) $HisQMP_2$ (●), HisJ (▲), $HisQMP_2$ in the presence of HisJ (◆), and mathematical sum of the spectra of $HisQMP_2$ and HisJ (○). Under these conditions the $HisQMP_2$ available for interaction is 71% saturated with HisJ [HisJ binds to $HisQMP_2$ with a K_d value = 10 mM (ref *21*)]. (B) Residual spectrum, i.e., difference between the experimental spectrum of $HisQMP_2$ in the presence of HisJ (◆) and the mathematical sum (○), as smoothed by the KaleidaGraph program. Panels C and D are the same as panels A and B but in the presence of L-histidine (0.1 mM) in the HisJ-containing samples.

defined above, does not appear to involve this residue, at least as detectable by this technique.

Conformational Changes As Observed by CD in the Far UV. The far-UV CD spectrum of a protein provides information about its secondary structure and can be used to detect structural rearrangements resulting from conformational changes. This technique is most sensitive to rearrangements in α-helical structures. $HisQMP_2$ is expected to undergo conformational changes upon its interactions with HisJ (the receptor), MgATP, and ligand. The far-UV CD spectrum of $HisQMP_2$ in PLS (Figure 6A, ●) is typical of a highly α-helical protein, as deduced from the presence of minima at 208 and 222 nm. A maximum at 195 nm (rather than at 190 nm, as is typical of an α-helical structure) suggests substantial contribution(s) from other secondary structural elements (*53*). The total α-helical content of the complex, F_h, as determined from the absolute value of ellipticity at 222 nm, $[\Theta]^{222}$ from the equation $F_h = -([\Theta]^{222} + 260)/35\,740$ (*54*), is 43.5% ± 5.2%.[6] This α-helical content is consistent with the value calculated for HisP from its resolved crystal structure (*19*) and for HisQ and HisM from sequence analysis (*10*).

Artifacts, such as light scattering and nonhomogeneity in the distribution of protein molecules (known as absorption flattening effects), could substantially affect the spectrum of membrane proteins (*53*, *55*−*57*). If such artifacts were present in the PLS_{crude} system, addition of detergent would eliminate them. OG at a concentration of 1.2% was chosen because the structure of $HisQMP_2$ is preserved in its presence, as demonstrated by the finding that $HisQMP_2$ binds several analogues of ATP, such as TNP-ATP (*25*) and 8-azido-ATP (*34*), and retains full activity, for both ATPase and transport (*17*, *18*). Addition of 1.2% OG has no effect on the far-UV CD spectrum of $HisQMP_2$ (data not shown), indicating the absence of the above artifacts. The effects of decreasing the protein/lipid ratio 4-fold while maintaining the lipid concentration constant and of changing the path length of the cell from 0.01 to 0.02 cm were also investigated. Neither resulted in spectral changes (data not shown). Thus, the shape of the spectrum of $HisQMP_2$ appears to be free of artifacts (*53*, *55*, *57*). All further data were collected in the absence of detergent.

The CD spectra of unliganded HisJ (▲) and of $HisQMP_2$ in the presence of 25 μM HisJ (◆) are shown in Figure 6A. The difference between the mathematical sum of the individual spectra of $HisQMP_2$ and of HisJ (○) and the spectrum obtained for $HisQMP_2$ in the presence of HisJ (♦) is shown in Figure 6B. It has a maximum at 192 nm, with an increase in ellipticity of 23%. An essentially identical differential spectrum is obtained if the receptor is liganded (Figure 6C,D). No significant effect is observed if 0.5 mM L-histidine or 0.5 mM MgATP [which binds to $HisQMP_2$ with an apparent affinity of 0.6 mM (*18*)] or both are added in the absence of HisJ (data not shown). Thus, the interaction of liganded or unliganded HisJ with $HisQMP_2$ (abortive signaling) is accompanied by secondary structure reorganization as detectable by far-UV CD spectroscopy. This rearrangement presumably occurs in $HisQMP_2$, although it may also involve HisJ upon its interaction with the complex. Given that liganded and unliganded HisJ yield the same effect, despite the dramatic difference between these two forms (*58*−*60*), it is likely that the observed change in the secondary structure involves mostly $HisQMP_2$. Measurements in the presence of both liganded HisJ and ATP, which results in ATP hydrolysis (productive signaling), are not possible due both to optical interference from the high concentration of ATP required and to the long time necessary for spectral data collection (about 1 h), during which time

[6] Mean of six samples, four independent preparations.

substantial consumption of ATP and accumulation of inhibitory ADP occurs (*17*).

Conformational Changes As Observed by Intrinsic Fluorescence. In tryptophan-containing proteins, the intrinsic fluorescence intensity is mostly determined by tryptophanyls (*61*). If tryptophan residues are located so that changes occur in their microenvironment, i.e., in nearby amino acid residues (within the distance of several angstroms; *62*−*64*), conformational changes could be detected as changes in intrinsic fluorescence. In $HisQMP_2$, each of the two HisP subunits contains a single tryptophan residue (Trp-105); HisQ and HisM contain two and five tryptophan residues, respectively; and the soluble receptor, HisJ, contains a single tryptophan residue, Trp-130. The $HisQMP_2$ spectrum has a peak at 337 nm (data not shown), which suggests that (some of) the tryptophanyls are in a hydrophobic environment.

To use changes in fluorescence intensity of $HisQMP_2$ to analyze the effect of the interaction with HisJ, the level of fluorescence of the latter must be negligible in comparison to that of $HisQMP_2$. However, the HisJ concentration necessary for efficient interaction with $HisQMP_2$ must be at least 10 μM, which would result in an unacceptably high fluorescence signal that would mask the $HisQMP_2$ signal. Raising the $HisQMP_2$ concentration above 1.0 μM to obviate this problem is not possible because of excessive light scattering. Therefore, a tryptophanless HisJ, W130F, was created by in vitro mutagenesis by replacing Trp-130 of HisJ with phenylalanine (see Experimental Procedures). W130F was shown to be identical to the wild type with respect to numerous biochemical and physiological properties: the K_d of W130 for L-histidine binding is 43 nM, which is experimentally indistinguishable from that of wild-type HisJ [30 nM (*59*)]; the affinity of L-histidine-liganded W130F for $HisQMP_2$ is 6 μM, which is similar to that of wild-type HisJ [10 μM (*18*, *21*)]; W130F induces the ATPase activity of $HisQMP_2$ in the absence of L-histidine to the same level as that induced by wild-type HisJ (*18*); and W130F supports D-histidine transport (*65*) through the $HisQMP_2$ complex in vivo as well as the wild type. The fluorescence emission spectrum of W130F upon excitation at 296 nm (at which wavelength mostly tryptophanyls are excited) was determined. Figure 7 shows that it has a flat maximum at 340 nm, which does not increase upon addition of L-histidine, in contrast to the behavior of wild-type HisJ.[7] Thus, W130F does not contribute significantly to fluorescence excited at 296 nm and has biochemical properties that are the same as those of the wild type, and it can be used to analyze whether, upon interaction, it induces conformational changes in $HisQMP_2$.

Figure 8 (line 1) shows the $HisQMP_2$ spectrum in the presence of 2 mM MgATP and in the absence of receptor, after correction for the inner filter effect.[8] This spectrum displays a lower fluorescence intensity (by about 5%) than in the absence of ATP (latter spectrum not shown). This decrease presumably reflects conformational changes due to ATP binding, which might occur in any of the subunits.[9]

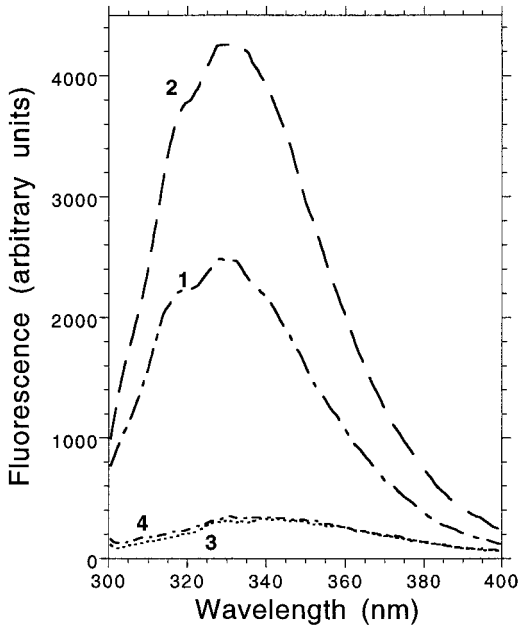

FIGURE 7: Intrinsic fluorescence emission spectra of wild-type HisJ and W130F. Measurements were performed in a 1.0 × 1.0 cm cell, with both slits set at 2 nm. HisJ (curves 1 and 2) and W130F (curves 3 and 4) were both 10 μM in 50 mM Tris-HCl, pH 8.0; L-histidine, when present (curves 2 and 4), was 0.1 mM.

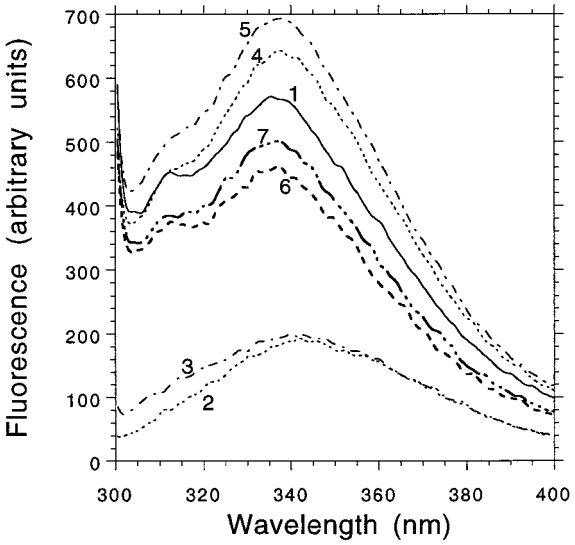

FIGURE 8: Effect of W130F on the intrinsic fluorescence spectrum of $HisQMP_2$ in the presence of MgATP. All samples contain 50 mM Tris-HCl buffer, pH 8.0, and 2 mM MgATP, plus the following components, if present: 1 μM $HisQMP_2$ in PLS_{crude}, 10 μM W130F, 0.1 mM L-histidine. Line 1, $HisQMP_2$; line 2, W130F; line 3, W130F and L-histidine; line 4, $HisQMP_2$ and W130F; line 5, $HisQMP_2$, W130F, and L-histidine. Lines 6 and 7 are calculated from spectra 4 and 5 by subtracting the receptor contribution given by spectra 2 and 3, respectively. All spectra are corrected for the corresponding buffer baselines. Measurements are performed in a 0.3 × 0.3 cm cell, with both slits set at 5 nm. The samples are prepared by freezing−thawing as described under Experimental Procedures. Line 1 displays a decrease of about 5% ± 2% in fluorescence intensity in the $HisQMP_2$ spectrum at 337 nm, with no peak shift, as compared to the same sample in the absence of ATP (spectrum not shown).

[7] Upon excitation at 280 nm (which excites both tyrosine and tryptophan fluorescence), W130F displays a peak with a maximum at 308 nm, which is typical of a tyrosine-containing, tryptophanless protein (*61*), the intensity of which increases linearly with increasing concentrations of L-histidine, up to a maximum of 21% when the histidine concentration equals that of W130F. The small peak with a flat maximum at about 340 nm, which does not increase in the presence of L-histidine, is presumably due to Trp-containing contaminant proteins. These data also confirm that W130F is unliganded (see Experimental Procedures).

Upon addition of either liganded or unliganded W130F to $HisQMP_2$ in the absence of ATP, the spectrum of $HisQMP_2$ is affected slightly (data not shown; in all cases the spectrum has been corrected for the fluorescence due to receptor alone). In three independent experiments there was a 4% ± 2% intensity decrease without a shift in the peak. Thus, abortive signaling results in minor structural changes that involve the tryptophan residues and that might occur in any of the $HisQMP_2$ subunits. The addition of both ATP and liganded W130F results in an increase in fluorescence intensity that is different from that obtained with ATP and unliganded W130F (Figure 8, lines 5 and 4, respectively). Correction of these spectra for the contribution by unliganded and liganded receptor alone (lines 2 and 3, respectively), results in lines 6 and 7, which display decreases of 12% ± 3% and 7% ± 2% at 337 nm, respectively, with no shift in the peak maximum, suggesting that the two forms send different signals. In fact, the decrease induced by unliganded receptor is larger than that by the liganded form (three independent experiments). Thus, changes occur (in any of the tryptophan residues in $HisQMP_2$) following productive signaling, even if only the intrinsic ATPase is induced. It is possible that the difference seen in conformational changes when the system is complete ($HisQMP_2$, the receptor, the ligand, and ATP, i.e., full productive signaling; line 5), as compared to those present in the absence of ligand (line 4), reflects specifically ATP hydrolysis and its consequences, (such as, for example, translocation and/or a return signal for the release of the receptor).

Conformational Changes As Observed by Fluorescence Quenching. Another approach to detect conformational changes involves quenching of tryptophanyl fluorescence with iodide anions. Quenching occurs if a tryptophan residue is exposed because I^- ions penetrate poorly the hydrophobic core of a protein and the lipid bilayer (*61*, *62*, *66*). The extent of quenching is described by the slope of the quenching curve by use of Stern−Volmer coordinates[10] and it is a measure of the exposure of the tryptophanyl(s) to the solvent; a change in such a slope reflects a conformational change (*66*). Figure 9A (○) shows that I^- ions quench the fluorescence of $HisQMP_2$, with 0.2 M KI resulting in a decrease of 12% (corresponding to a value of F_0/F of 1.14 in the Stern−Volmer plot). Increasing the KI concentration further has only a small additional effect. The leveling off of the quenching curve suggests that the tryptophanyls are classifiable in two groups: exposed to the solvent and buried (*61*). Of all the tryptophanyls present in $HisQMP_2$, Trp-105 in HisP is 80% exposed (*19*), while Trp-158 in HisQ and Trp-28 in HisM are likely to be inaccessible, being in the middle of hydrophobic membrane-spanning stretches (*10*). Given that Trp-105 is present in two copies and is partially

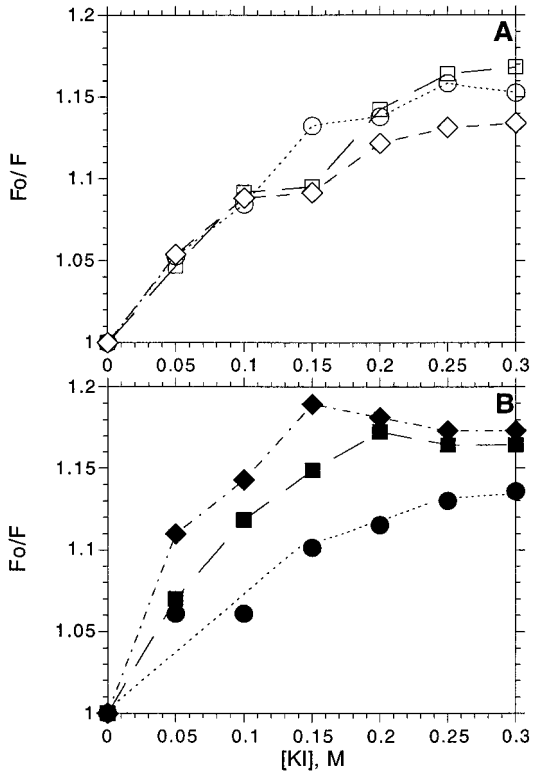

FIGURE 9: I^- ion quenching of the intrinsic fluorescence of $HisQMP_2$. The reaction is performed in 50 mM Tris-HCl buffer, pH 8.0, containing 1 μM $HisQMP_2$ in PLS_{crude}. Additions, when present, are (final concentrations) 10 μM W130F, 0.1 mM L-histidine, and 2 mM MgATP. KI and KCl are added at the indicated final concentrations (abscissa), as described under Experimental Procedures. The fluorescence intensity at 337 nm at zero concentration of KI (F_0) and at various KI concentrations (F) is obtained from the $HisQMP_2$ spectrum and corrected for the respective baseline and for the presence of the receptor, as described in Figure 8. Measurements are performed in a 0.3 × 0.3 cm cell, with both slits set at 5 nm. Quenching of fluorescence of $HisQMP_2$ is measured in the absence (A) or presence (B) of MgATP. Circles, no additions; squares, W130F; diamonds, W130F and L-histidine. The results shown were obtained in a single experiment, with each sample point done in triplicate (SD is ±0.01); three independent experiments were performed, which gave essentially identical results.

exposed, at least as it appears in the crystal structure (*19*), it appears likely that the changes observed reflect at least movement of these residues. Flattening of the curve may reflect, at least in part, the inaccessibility of Trp-158 and Trp-28 (in HisQ and HisM, respectively). The addition of ATP does not change the slope at KI concentrations below 0.1 M (compare ○ in Figure 9A with ● in Figure 9B), whereas a small difference is apparent at concentrations higher than 0.1 M KI. Addition of unliganded or liganded receptor (W130F) in the absence of ATP (abortive signaling) causes small changes (Figure 9A, □ and ◇, respectively), which might reflect minor conformational changes, corresponding to those detected by intrinsic fluorescence measurements. If ATP is present in addition to unliganded receptor (productive signaling for the intrinsic ATPase), the quenching curve has a steeper slope and a higher final level than in its absence (Figure 9B; compare ■ with ●). Liganded W130F in the presence of ATP (♦) results in a slope that is even steeper than that with unliganded receptor, although the final levels are similar. Thus, in agreement with the conclusions

[8] The inner filter effect of MgATP is taken into account by correction of the observed fluorescence intensity according to the formula $F_{corr} = F_{obs}$ antilog($OD_{296nm}/2$) (*61*), where OD_{296nm} is the optical density at 296 nm of the MgATP solution measured in the same cell (0.3 × 0.3 cm).

[9] It is also possible that slow ATP hydrolysis via the intrinsic ATPase activity (*18*) contributes at least in part to these changes.

[10] The Stern−Volmer coordinates are the reversed relative fluorescence intensity and the quencher concentration; a linear dependence is generally indicative of a single class of fluorophores, all equally accessible to quencher. Such an analysis also eliminates the contribution of the inner filter effect of ATP.

from the intrinsic fluorescence measurements, when the system is complete, significant conformational changes appear to occur that increase the accessibility of at least some of the tryptophan residues in $HisQMP_2$ and are different whether the ATPase activity is intrinsic or fully induced.

DISCUSSION

We chose to use sulfhydryl reagents as tools to initiate a study of conformational changes and of the nature of the two identical HisP subunits within the intact complex. We specifically wished to analyze these aspects without altering the complement of cysteine residues by in vitro mutagenesis. This approach was made possible because (i) there is a single cysteine residue in HisP, (ii) we established that this residue is not necessary for enzymatic action, and (iii) we developed a method to resolve the sulfhydryl-modified HisP and quantitate its level of modification.

The histidine transporter presents an interesting problem with regard to the nature of the NBDs, which are identical in sequence but are here shown to behave differently with respect to their reactivity with thiol-specific reagents. We already excluded a number of artifactual possibilities. Here we consider a few additional ones. Our findings obtained with PyMPO, qBBr, and mBBr might reflect the loss of reactivity in one of the NBDs by the prior modification of the other (a form of negative cooperativity), possibly through steric hindrance by the one reacted NBD or a change in the electric field in the vicinity of the as-yet-unreacted Cys-51. However, these explanations are questionable because MIANS is as bulky as PyMPO and bulkier than qBBr, yet it modifies both sites, and mBBr is not charged and therefore should be insensitive to charge changes. In any case, important structural changes resulting from PyMPO modification at one site are unlikely because the second site maintains reactivity toward MIANS. Thus, the asymmetry may be intrinsic to the structure of the complex, for example, through the interaction of the HisP molecules with HisQ and HisM. However, it is also possible that the HisP subunits take different conformations within the HisP dimer independently of interactions with other elements and/or specifically as part of a functional cycle, e.g., upon ATP binding, ATP hydrolysis and/or the release of its products, or substrate translocation.

The notion that NBDs in ABC transporters are functionally different is consistent with a number of findings obtained in a variety of such systems. In prokaryotes, the demonstration of positive cooperativity for ATP in the histidine and maltose permeases supports the concept of separable functions for the two domains (*18*, *67*), and so do data indicating that the HisP subunits function in alternating fashion, with one of them activating the other to hydrolyze ATP (*23*). In the case of eukaryotes, the NBDs are often not identical in sequence, thus providing a structural explanation for the functional asymmetry. Some examples of functional differences between the NBDs of eukaryotes are the different behavior of the NBDs of MDR (*68*), the alternating mechanism proposed for the NBDs of MDR (*69*, *70*), the asymmetry observed in the electrophysiological signal in CFTR (*71*), and the different behavior in CFTR of the two NBDs with respect to nucleotide hydrolysis (*72*). However, it is interesting that, in the case of MDR, the two NBDs do not display any structural differences as determined by use of fluorescent sulfhydryl reagents (*73*). If the identical (sequence-wise) NBDs of the histidine permease are indeed intrinsically different, it would imply that asymmetry is an essential property of NBDs. The structural basis of the asymmetry in the histidine transporter is not yet obvious.

Table 1: Changes Detected in $HisQMP_2$

changes upon	α-helix[a]	dynamics in the system[d]	local change (Cys-51)
signaling[c]	+	+[b]	−
ATP binding	−	+[b]	+
full activity	nd[e]	+[b]	+

[a] By far-UV CD. [b] Changes differ from each other. [c] Abortive and productive. [d] By tryptophan fluorescence. [e] Not determined.

A summary of the results obtained with a combination of various approaches to study conformational changes is shown in Table 1. Some secondary structural changes are observed in the far-UV CD spectrum upon interaction of the complex with the receptor in the absence of ATP, when some transmembrane signaling is expected to occur (although additional reorganization would take place if the system were complete). The finding that the maximum of the residual spectrum is at 192 nm (Figure 6) suggests that the conformational change has occurred in an α-helical structure within $HisQMP_2$. Although HisQ and HisM would be obvious participants in this reorganization, it is likely that HisP also participates because it is partially inserted into the membrane (*74*) and interacts with HisQ and HisM (*22*, *34*, *74*; unpublished results). In particular, since membrane-spanning α-helices (in HisQ and HisM) typically behave like rigid bodies (*36*, *75*, *76*), we speculate that the changes observed by UV CD occur specifically in HisP. A possible candidate for such changes would be the helical domain of HisP. It is interesting that the observed changes are the same whether the receptor is liganded or not, indicating that the complex responds whether it is able to complete the cycle of transport or not. This is consistent with the finding that the affinity of the receptor for the complex is the same whether it is liganded or not and the initial receptor response is the same (*21*). Additional conformational changes presumably occur in this secondary structure and/or in additional ones when both ATP and liganded receptor are present; they could not be measured by far-UV CD for technical reasons, but may be at the basis of the changes observed by tryptophan fluorescence quenching. No changes were observed by UV CD upon ATP binding in the absence of receptor, which would suggest that α-helices do not change conformation, or change only minimally, upon ATP binding. It should be noted that in the case of MalK, the NBD of the maltose periplasmic permease, limited proteolysis experiments have shown changes occurring upon ATP binding that have led to the suggestion that it is the helical domain that undergoes conformational changes (*77*). The changes detected in MalK by this methodology may also be of a tertiary nature, by analogy to HisP.

The existence of tertiary structural conformational changes was also analyzed. In the absence of ATP, modest changes are observed upon signaling, by both fluorescence and fluorescence quenching. No changes are observed with sulfhydryl modification, indicating that the cysteines are not

involved in signaling. Some clear tertiary structural conformational changes occur upon ATP binding (in the absence of receptor), as shown by fluorescence and fluorescence quenching, and they are larger if both ATP and receptor are present. Tertiary changes are also likely to be responsible for those detected upon ATP binding by sulfhydryl modification; these were determined to occur specifically in HisP. Thus, it appears that the α-helix in which Cys-51 is located (following the nucleotide-binding loop) is involved in tertiary structural changes but not in secondary structure ones, since no significant changes are detected by CD measurements. In this respect it is also interesting that although conformational changes are larger when the system is complete, i.e., fully active, as determined by fluorescence quenching, there are no equivalent larger changes in the modification of Cys-51 in HisP. We speculate that the relatively slow rate of the ATPase (the turnover rate is in the range 0.1−10 s^{-1}; see ref *14* and references therein) results in the nucleotide-binding pocket(s) being occupied most of the time in the cycle. It should be noted that the difference in fluorescence quenching between full productive signaling and intrinsic ATPase signaling (i.e., ATP and liganded receptor versus ATP and unliganded receptor; Figure 9B) indicates that translocation per se is accompanied by additional conformational changes. In this respect, it has been suggested that larger global changes in the tertiary structure of MDR occur with a full catalytic cycle (*78*). Overall, complex conformational changes occur in the translocation cycle as measured by these methods. In particular, from the three-dimensional structure of HisP (*19*), it can be seen that Cys-51 is located in α-helix 1, which is close to the ATP-binding pocket and thus may reflect changes originating in this pocket. Cys-51 is also close to a series of *β*-strands that connect the binding pocket with the helical domain (arm II of the structure, interacting with HisQ/M); thus we speculate that movement of Cys-51 might be part of a signaling relay between ATP hydrolysis and the function of the rest of the transporter.

In conclusion, by careful analysis of this system at various functional states and with different techniques we were able to demonstrate that such states are associated with the accumulation of particular conformational species. Comparison of various steady-state conditions provides insights into the nature of conformational changes associated with individual steps in a cycle of activity. In addition, these studies have provided evidence supporting previous conclusions regarding the following structural properties: the percentage of α-helical structures and the topology of the hydrophobic membrane spanners, HisQ and HisM (*10*); the similarity of organization between HisP in solution and HisP in the complex [by showing the extremely poor accessibility of Cys-51 in the complex, thus confirming its location in the X-ray crystal structure of soluble HisP (*19*)]; the previously suspected asymmetry of the two HisP subunits (*13*, *14*, *18*); and the postulated increase in the dynamics of the system under conditions of full activity (*5*, *79*).

Finally, detection of conformational changes in membrane systems is generally difficult. Few ABC transporters have been purified and had their biochemical properties analyzed; therefore, it is relatively difficult to make extensive comparisons. In the case of purified and reconstituted MDR, tertiary structure changes comparable to those presented here were also observed upon ATP binding by D/H exchange rate measurements and fluorescence quenching (*80*). The development of the techniques presented in this paper should be helpful in similar studies with other ABC transporters.

ACKNOWLEDGMENT

We thank G. Wang for help in site-directed mutagenesis work; S. Zhang for performing transport assays; D. Caseñas for help in the purification and characterization of the membrane complex and for performing some of the ATPase measurements; P.-Q. Liu and C. E. Liu for providing purified $HisQMP_2$ in the early stages of this work and for valuable discussions; D. G. Drubin and S. Marqusee for the use of the spectrofluorometer and spectropolarimeter, respectively; and L.-W. Hung, A. F. Kolodziej, and K. Nikaido for valuable discussions.

REFERENCES

1. Ames, G. F.-L., Mimura, C., and Shyamala, V. (1990) *FEMS Microbiol. Rev. 75*, 429−446.
2. Hyde, S. C., Emsley, P., Hartshorn, M. J., Mimmack, M. M., Gileadi, U., Pearce, S. R., Gallagher, M. P., Gill, D. R., Hubbard, R. E., and Higgins, C. F. (1990) *Nature 346*, 362−365.
3. Rust, S., Rosier, M., Funke, H., Real, J., Amoura, Z., Piette, J.-C., Deleuze, J.-F., Brewer, H. B., Duverger, N., Denefle, P., and Assmann, G. (1999) *Nat. Genet. 22*, 352−355.
4. Allikmets, R., Singh, N., Sun, H., Shroyer, N. F., Hutchinson, A., Chidambaram, A., Gerrard, B., Baird, L., Stauffer, D., Peiffer, A., Rattner, A., Smallwood, P., Li, Y., Anderson, K. L., Lewis, R. A., Nathans, J., Leppert, M., Dean, M., and Lupski, J. R. (1997) *Nat. Genet. 15*, 236−246.
5. Doige, C. A., and Ames, G. F.-L. (1993) *Annu. Rev. Microbiol. 47*, 291−319.
6. Ames, G. F.-L. (1985) *Curr. Top. Membr. Transp. 23*, 103−119.
7. Ames, G. F.-L., Mimura, C., Holbrook, S., and Shyamala, V. (1992) *Adv. Enzymol. Relat. Areas Mol. Biol. 65*, 1−47.
8. Ehrman, M., Ehrle, R., Hofmann, E., Boos, W., and Schlosser, A. (1998) *Mol. Microbiol. 29*, 685−694.
9. Kerppola, R. E., Shyamala, V., Klebba, P., and Ames, G. F.-L. (1991) *J. Biol. Chem. 266*, 9857−9865.
10. Kerppola, R. E., and Ames, G. F.-L. (1992) *J. Biol. Chem. 267*, 2329−2336.
11. Joshi, A., Ahmed, S., and Ames, G. F.-L. (1989) *J. Biol. Chem. 264*, 2126−2133.
12. Ames, G. F.-L. (1990) *Res. Microbiol. 141*, 341−348.
13. Liu, P.-Q., and Ames, G. F.-L. (1998) *Proc. Natl. Acad. Sci. U.S.A. 95*, 3495−3500.
14. Nikaido, K., Liu, P.-Q., and Ames, G. F.-L. (1997) *J. Biol. Chem. 272*, 27745−27752.
15. Petronilli, V., and Ames, G. F.-L. (1991) *J. Biol. Chem. 266*, 16293−16296.
16. Speiser, D. M., and Ames, G. F.-L. (1991) *J. Bacteriol. 173*, 1444−1451.
17. Liu, C. E., and Ames, G. F.-L. (1997) *J. Biol. Chem. 272*, 859−866.
18. Liu, C. E., Liu, P.-Q., and Ames, G. F.-L. (1997) *J. Biol. Chem. 272*, 21883−21891.
19. Hung, L.-W., Wang, I. X., Nikaido, K., Liu, P.-Q., Ames, G. F.-L., and Kim, S.-H. (1998) *Nature 396*, 703−707.
20. Mimura, C. S., Holbrook, S. R., and Ames, G. F.-L. (1991) *Proc. Natl. Acad. Sci. U.S.A. 88*, 84−88.
21. Ames, G. F.-L., Liu, C. E., Joshi, A. K., and Nikaido, K. (1996) *J. Biol. Chem. 271*, 14264−14270.
22. Liu, P.-Q., Liu, C. E., and Ames, G. F.-L. (1999) *J. Biol. Chem. 274*, 18310−18318.
23. Nikaido, K., and Ames, G. F.-L. (1999) *J. Biol. Chem. 274*, 26727−26735.
24. Lever, J. E. (1972) *J. Biol. Chem. 247*, 4317−4326.

25. Liu, C. E. (1996) Ph.D. Thesis University of California at Berkeley.
26. Kang, C., Kim, S.-H., Nikaido, K., Gokcen, S., and Ames, G. F.-L. (1989) *J. Mol. Biol. 207*, 643−644.
27. Nikaido, K., and Ames, G. F.-L. (1992) *J. Biol. Chem. 267*, 20706−20712.
28. Lowry, O. H., Rosebrough, N. J., Farr, A. L., and Randall, R. J. (1951) *J. Biol. Chem. 193*, 265−275.
29. Lever, J. E. (1972) *Anal. Biochem. 50*, 73−83.
30. Peterson, G. L. (1977) *Anal. Biochem. 83*, 346−356.
31. Haugland, R. P. (1996) *Handbook of Fluorescent Probes and Research Chemicals*, 6th ed., Molecular Probes, Inc., Eugene, OR.
32. Hobson, A., Weatherwax, R., and Ames, G. F.-L. (1984) *Proc. Natl. Acad. Sci. U.S.A. 81*, 7333−7337.
33. O'Keefe, D. O. (1994) *Anal. Biochem. 222*, 86−94.
34. Mimura, C. S., Admon, A., Hurt, K. A., and Ames, G. F.-L. (1990) *J. Biol. Chem. 265*, 19535−19542.
35. Cecil, R., and McPhee, J. R. (1959) *Adv. Protein Chem. 14*, 225−389.
36. Farrens, D. L., Altenbach, C., Yang, K., Hubbell, W. L., and Khorana, H. G. (1996) *Science 274*, 768−770.
37. Akabas, M. H., Stauffer, D. A., Xu, M., and Karlin, A. (1992) *Science 258*, 307−310.
38. Yan, R.-T., and Maloney, P. C. (1995) *Proc. Natl. Acad. Sci. U.S.A. 92*, 5973−5976.
39. Keller, R. C. A., ten Berge, D., Nouwen, N., Snel, M. M. E., Tommassen, J., Marsh, D., and de Kruijff, B. (1996) *Biochemistry 35*, 3063−3071.
40. Mannuzzu, L. M., Moronne, M. M., and Isacoff, E. Y. (1996) *Science 271*, 213−216.
41. Altenbach, C., Yang, K., Farrens, D. L., Farahbakhsh, Z. T., Khorana, H. G., and Hubbell, W. L. (1996) *Biochemistry 35*, 12470−12478.
42. Ottemann, K. M., Xiao, W., Shin, Y. K., and Koshland, D. E., Jr. (1999) *Science 285*, 1751−1754.
43. Lu, J., Baase, W. A., Muchmore, D. C., and Dahlquist, F. W. (1992) *Biochemistry 31*, 7765−7772.
44. Kreimer, D. I., Dolginova, E. A., Raves, M., Sussman, J. L., Silman, L., and Weiner, L. (1994) *Biochemistry 33*, 14407−14418.
45. Shin, I., Kreimer, D., Silman, I., and Weiner, L. (1997) *Proc. Natl. Acad. Sci. U.S.A. 94*, 2848−2852.
46. Weitzman, C., Consler, T. G., and Kaback, H. R. (1995) *Protein Sci. 4*, 2310−2318.
47. Liu, R., and Sharom, F. J. (1998) *Biochemistry 37*, 6503−6512.
48. Higgins, C. F., Haag, P. D., Nikaido, K., Ardeshir, F., Garcia, G., and Ames, G. F.-L. (1982) *Nature 298*, 723−727.
49. Kosower, N. S., and Kosower, E. M. (1987) *Methods Enzymol. 143*, 77−84.
50. Shyamala, V., Baichwal, V., Beall, E., and Ames, G. F.-L. (1991) *J. Biol. Chem. 266*, 18714−18719.
51. Oh, B.-H., Kang, C.-H., De Bondt, H., Kim, S.-H., Nikaido, K., Joshi, A., and Ames, G. F.-L. (1994) *J. Biol. Chem. 269*, 4135−4143.
52. Yao, N., Trakhanov, S., and Quiocho, F. A. (1994) *Biochemistry 33*, 4769−4777.
53. Woody, R. W. (1995) *Methods Enzymol. 246*, 34−71.
54. Batra, P. P., Roebuck, M. A., and Uetrecht, D. (1990) *J. Protein Chem. 9*, 37−44.
55. Foster, D. L., Boublik, M., and Kaback, H. R. (1983) *J. Biol. Chem. 258*, 31−34.
56. Gibson, A. L., Wagner, L. M., Collins, F. S., and Oxender, D. L. (1991) *Science 254*, 109−111.
57. Heyn, M. P. (1989) *Methods Enzymol. 172*, 575−584.
58. Wolf, A., Shaw, E. W., Nikaido, K., and Ames, G. F.-L. (1994) *J. Biol. Chem. 269*, 23051−23058.
59. Wolf, A., Lee, K. C., Kirsch, J. F., and Ames, G. F.-L. (1996) *J. Biol. Chem. 271*, 21243−21250.
60. Oh, B.-H., Pandit, J., Kang, C.-H., Nikaido, K., Gokcen, S., Ames, G. F.-L., and Kim, S.-H. (1993) *J. Biol. Chem. 268*, 11348−11353.
61. Lakowicz, J. R. (1983) *Introduction to fluorescence spectroscopy*, Plenum Press, New York.
62. Lakowicz, J. R., Zelent, B., Gryczynski, I., Kusba, J., and Johnson, M. L. (1994) *Photochem. Photobiol. 60*, 205−214.
63. Gopalan, V., Golbik, R., Schreiber, G., Fersht, A. R., and Altman, S. (1997) *J. Mol. Biol. 267*, 765−769.
64. Chen, Y., and Barkley, M. D. (1998) *Biochemistry 37*, 9976−9982.
65. Ames, G. F.-L., Noel, K. D., Taber, H., Spudich, E. N., Nikaido, K., Afong, J., and Ardeshir, F. (1977) *J. Bacteriol. 129*, 1289−1297.
66. Eftink, M. R. (1991) in *Topics in Fluorescence Spectroscopy* (Lakowicz, J. R., Ed.) pp 53−126, Plenum Press, New York.
67. Davidson, A. L., Laghaeian, S. S., and Mannering, D. E. (1996) *J. Biol. Chem. 271*, 4858−4863.
68. Beaudet, L., and Gros, P. (1995) *J. Biol. Chem. 270*, 1−12.
69. Senior, A. E., Al-Shawi, M. K., and Urbatsch, I. L. (1995) *FEBS Lett. 377*, 285−289.
70. Hrycyna, C. A., Ramachandra, M., Ambudkar, S. V., Ko, Y. H., Pedersen, P. L., Pastan, I., and Gottesman, M. M. (1998) *J. Biol. Chem. 273*, 16631−16634.
71. Gunderson, K. L., and Kopito, R. R. (1995) *Cell 82*, 231−239.
72. Gadsby, D. C., and Nairn, A. C. (1999) *Physiol Rev. 79*, S77−S107.
73. Sharom, F. J., Liu, R., Romsicki, Y., and Lu, P. (1999) *Biochim. Biophys. Acta 1461*, 327−345.
74. Baichwal, V., Liu, D., and Ames, G. F.-L. (1993) *Proc. Natl. Acad. Sci. U.S.A. 90*, 620−624.
75. Milburn, M. V., Prive, G. G., Milligan, D. L., Scott, W. G., Yeh, J., Jancarik, J., Koshland, D. E., Jr., and Kim, S. H. (1991) *Science 254*, 1342−1347.
76. Ottemann, K. M., Thorgeirsson, T. E., Kolodziej, A. F., Shin, Y.-K., and Koshland, D. E., Jr. (1998) *Biochemistry 37*, 7062−7069.
77. Mourez, M., Jehanno, M., Schneider, E., and Dassa, E. (1998) *Mol. Microbiol. 30*, 353−363.
78. Sharom, F. J., Liu, R., and Romsicki, Y. (1998) *Biochem. Cell Biol. 76*, 695−708.
79. Ames, G. F.-L. (1993) *Int. Rev. Cytol. 137a*, 1−35.
80. Sonveaux, N., Shapiro, A. B., Goormaghtigh, E., Ling, V., and Ruysschaert, J.-M. (1996) *J. Biol. Chem. 271*, 24617−24624.

BI001066+